

Fast and High-Strain Electrochemically Driven Yarn Actuators in Twisted and Coiled Configurations

Shazed Aziz, Jose G. Martinez, Bidita Salahuddin, Nils-Krister Persson, and Edwin W. H. Jager*

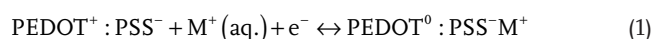
Commercially available yarns are promising precursor for artificial muscles for smart fabric-based textile wearables. Electrochemically driven conductive polymer (CP) coated yarns have already shown their potential to be used in smart fabrics. Unfortunately, the practical application of these yarns is still hindered due to their slow ion exchange properties and low strain. Here, a method is demonstrated to morph poly-3,4-ethylenedioxythiophene:poly-styrenesulfonate (PEDOT:PSS) coated multifilament textile yarns in highly twisted and coiled structures, providing >1% linear actuation in <1 s at a potential of +0.6 V. A potential window of +0.6 V and −1.2 V triggers the fully reversible actuation of a coiled yarn providing >1.62% strain. Compared to the untwisted, regular yarns, the twisted and coiled yarns produce >9× and >20× higher strain, respectively. The strain and speed are significantly higher than the maximum reported results from other electrochemically operated CP yarns. The yarn's actuation is explained by reversible oxidation/reduction reactions occurring at CPs. However, the helical opening/closing of the twisted or coiled yarns due to the torsional yarn untwisting/re-twisting assists the rapid and large linear actuation. These PEDOT:PSS coated yarn actuators are of great interest to drive smart textile exoskeletons.

1. Introduction

Recently, textile yarns have become of great interest for use in artificial muscles.^[1] Several textile actuator configurations such as knitted


or woven structures were made using these yarns.^[2] The use of conductive polymer coatings on these yarns provided a new dimension in electrochemically operated artificial muscles. The electrochemically induced actuation mechanism of conductive polymer-based actuator rests on the volume alteration property of conductive polymer during the reversible doping/dedoping process. Introducing a small voltage (typically in the range of only a few volts) causes the electrons to be donated (oxidation) or accepted (reduction) by the conductive polymer chain. Anions and cations, including solvent molecules, in the surrounding electrolyte migrate between the conductive polymer and the external electrolyte to neutralize the charge in the conductive polymer, resulting in the expansion or contraction of the polymer electrodes, causing the geometric deformation of the actuator.^[3]

The conventional synthesis process of conductive polymers such as poly-3,4-ethylenedioxythiophene (PEDOT) is oxidative polymerization during which the material is also doped/oxidized.^[4] Anions are incorporated during this synthesis to compensate for the oxidation charge on the polymer backbone.^[5] The size of the charge-neutralizing counterion/dopant in the polymer chain included during synthesis as well as the size of the ions in the electrolyte during actuation determines the extent of volume change.^[3b,6] When the anions that are trapped during the synthesis are large such as poly-styrenesulfonate (PSS) or dodecylbenzenesulfonate (DBS), these anions become trapped within the polymer matrix and cannot leave when PEDOT is reduced. Here, cation-driven migration occurs from the solution to the PEDOT:PSS to compensate for the negative charges, which causes the material to expand driven by the reaction (1). Application of a positive voltage causes the oxidation of the polymer, generating polarons along conducting polymer chains and changing the distribution of the double bonds in the polymeric chains which drives the conformational movements of the chains. Such movements allow the mobile cations to be expelled to the surrounding electrolyte to keep the electroneutrality in the material and the PEDOT:PSS shrinks.^[7] This reversible process can be represented by the following driving reaction (here, PEDOT⁰ represents the neutral polymer chain, PEDOT⁺ the oxidized polymer chain, M⁺ is the cations exchanged during oxidation/reduction, and e[−] are the electrons):^[8]



Dr. S. Aziz, Dr. J. G. Martinez, Dr. E. W. H. Jager
Division of Sensor and Actuator Systems
Department of Physics, Chemistry, and Biology (IFM)
Linköping University
Linköping SE-581 83, Sweden
E-mail: edwin.jager@liu.se

Dr. B. Salahuddin
Australian Institute for Innovative Materials
University of Wollongong
Innovation Campus, Squires Way, North Wollongong, NSW 2522, Australia
Dr. N.-K. Persson
Smart Textiles Technology Lab
Swedish School of Textiles
University of Borås
Borås SE-501 90, Sweden

 The ORCID identification number(s) for the author(s) of this article can be found under <https://doi.org/10.1002/adfm.202008959>.

© 2020 The Authors. Advanced Functional Materials published by Wiley-VCH GmbH. This is an open access article under the terms of the Creative Commons Attribution-NonCommercial License, which permits use, distribution and reproduction in any medium, provided the original work is properly cited and is not used for commercial purposes.

DOI: 10.1002/adfm.202008959

Considering the electrochemically induced volume change of PEDOT:PSS, it is possible to harvest electrochemical actuation when the polymer is coated onto the surface of low-stiffness textile yarns.^[1c,2a,9] Impregnation of the conductive polymer in between the filaments of multifilament type yarns could contribute to the proper utilization of full-thickness volume alteration for harvesting the actuation properties. In addition to the materials perspective, amplification of actuation properties of the PEDOT:PSS impregnated textile yarns could be possible by means of introducing hierarchical structures such as twists and coils. Geometrically formed twisted or twist-induced coiled yarn structures could provide better actuation properties compared to untwisted ones.^[10]

The electrochemical actuation mechanism of twisted/coiled yarn actuators is also dependent on the ion-driven volumetric expansion/contraction of the constructing material when actuated.^[11] These unique helical structures take advantage of converting the radial contraction/expansion of the yarn material to the linear direction of the actuator resulting in an amplified linear actuation.^[12]

We here demonstrate novel PEDOT:PSS impregnated polyamide (PA6) multifilament textile yarns (PEDOT:PSS-PA6) that utilize the electrochemically driven volume change of PEDOT:PSS and that are helically twisted and coiled to harvest an amplified actuation magnitude when electrochemically activated. These yarns could be utilized as the building blocks in fabrics as electrochemomechanically active components of smart textiles and soft exoskeletons.

2. Results and Discussion

2.1. Electrochemical Characteristics

Cyclic voltammetry (CV) tests were performed by cycling the potential between 0.6 and −1.2 V for both twisted and coiled yarns in aqueous 0.1 M NaDBS electrolyte. CV measurements of the PEDOT:PSS-PA6 yarn actuators showed significant current under such protentional difference (**Figure 1**). Redox peaks observed in the CV curves shows that PEDOT behaves in agreement with prior results^[13] and pointed to the presence of a significant amount of electrochemically active polymer on the yarn surface, able to oxidize and reduce in these conditions. **Figure 1A-I** shows that the increase of the number of yarn plies in the twisted structures increased both the anodic and cathodic peaks indicating the higher amount of PEDOT:PSS. Similar trend is also observed from **Figure 1B-I** where the ratio of PEDOT:PSS to number of yarn plies in coiled actuators remained similar to the twisted ones. **Figure 1AII,BII** shows the coulombic cycles of twisted and coiled yarn actuators, respectively. Slight irreversibility of charge/potential curves was noticed during oxidation/reduction cycles, which possibly resulted from the irreversible side reactions such as water hydrolysis from the aqueous electrolyte media.^[14] **Figure 1C** shows the linear increase of current and charge when the loading of PEDOT:PSS is linearly increased (250, 500, 1000, and 1500 $\mu\text{L m}^{-1}$ PEDOT:PSS for core 1, 2, 4 and 6 ply yarns, respectively). This can be explained by the phenomenon that when the amount of conductive polymer is increased more material is available to be oxidized/reduced.^[15] The peak current keeps

increasing with the increased amount of PEDOT:PSS and shows a quick current response to the voltage change at both positive and negative vertex potential, illustrating the good electrochemical characteristics of the conductive yarn.

2.2. Surface Morphology

The surface morphology of the yarn actuators was characterized by using optical imaging and scanning electron microscopy (SEM). Moreover, energy-dispersive X-ray (EDX) spectroscopy was used to evaluate the elemental characteristics of the yarn actuators. The as-received PA6 yarn (**Figure 2A**) is bulky and the filaments are not compact (unless stress is applied) to form a multifilament yarn of uniform thickness. The coating of PEDOT:PSS gave a degree of compactness which is visually noticeable from surface uniformity and individual filament thickness, as shown in **Figure 2B**. The uniformity of yarn thickness throughout the whole length is crucial for having scalable actuation while the yarns are formed into twisted or coiled muscles.

The surface coverage and morphology study of the PEDOT:PSS-PA6 yarns having different number of yarn plies are important for determining the relative performance. **Figure 3A** shows the SEM images of twisted and coiled muscle PEDOT:PSS-PA6 yarns. Although the PEDOT:PSS loading seems to provide uniform coating on twisted yarns regardless of the number of plies, it significantly changes the coiled yarns morphology. As can be seen for 1 ply and 2 ply coiled yarns, lower amount of PEDOT:PSS did not affect the separation of each loop of coils, which is crucial for the actuation ability of coiled actuators.^[16] Although the higher loading of PEDOT:PSS (e.g., in 4 ply or 6 ply coiled yarns) uniformly coated the yarn, the conductive material was also suspended in between the individual coil loops. **Figure 3B** shows the EDX analysis of a sample 2 ply yarn actuators. The formation of a uniform PEDOT:PSS coating on the PA6 yarns was verified by the EDX spectra (right portion of **Figure 3B**) showing C, O and S with their intensity in agreement with the expected composition of the polymer.^[17] The significant rise of sodium peak points to the incorporation of Na^+ during electrochemical actuation as the mobile counter ion exchanged to keep the electroneutrality. The EDX elemental mapping (left portion of **Figure 3B**) of the yarn actuators verifies that elements C, O, and S are evenly covered on the coated area suggesting the uniform coverage of the PEDOT:PSS coating on the yarn.^[18]

2.3. Actuation Test Results

Electrochemically induced linear actuation of the PEDOT:PSS-PA6 regular, twisted, and coiled yarn actuators was performed in 0.1 M NaDBS aqueous solution. First, the actuation from a regular, untwisted/uncoiled 2 ply PEDOT:PSS-PA6 yarn was tested using consecutive square potential waves between −1.2 V (kept for 300 s) to 0.6 V (kept again for 300 s) versus Ag/AgCl. The regular yarn actuator produced 0.08% reversible linear contraction/expansion when positive/negative potential was applied, respectively. This actuation strain is similar to previous results reported by Maziz et al.^[2a] **Figure 4**

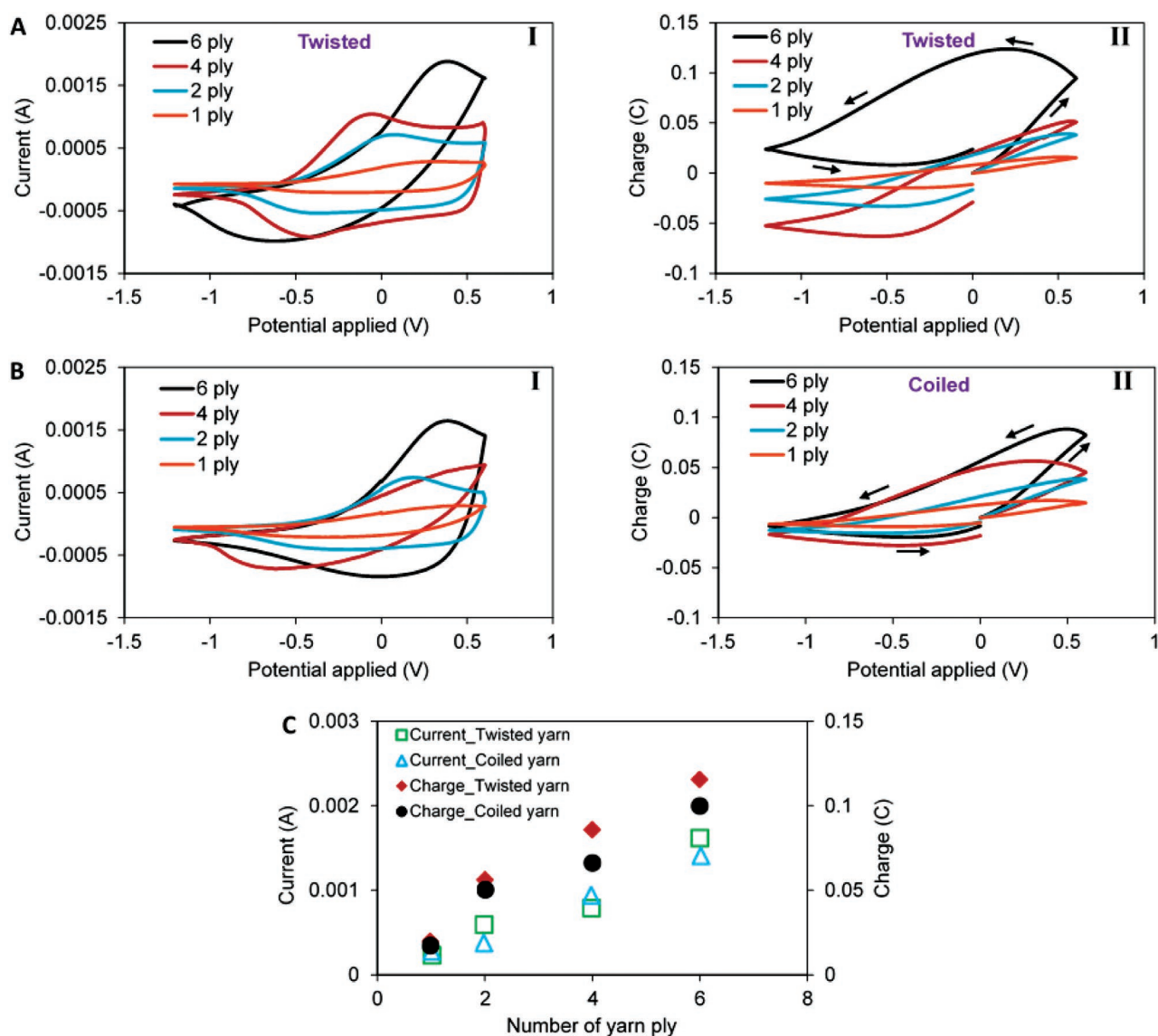


Figure 1. Cyclic voltammetry (I) and coulombic cycles (II) of yarn actuators obtained at 10 mV s^{-1} in 0.1 M NaDBS aqueous solution: A) 60 mm long twisted yarns, B) 25 mm long coiled yarns. C) Comparison of the flow of current flow (left y-axis) and reversible redox charge (right y-axis) through twisted and coiled yarns in terms of the number of yarn plies.

shows five consecutive cycles of the linear, tensile actuation obtained from twisted actuators composed of (A) 1 ply, (B) 2 ply, (C) 4 ply, and (D) 6 ply PA6 PEDOT:PSS-PA6 yarn. All the twisted PEDOT:PSS-PA6 yarns showed reversible tensile

actuation of 0.16%, 0.71%, 0.49% and 0.3% respectively under the same electrochemical conditions. Some creeping effect of the actuation strains was noticed, particularly in Figure 4B,C. This could be due partially to parallel irreversible reactions

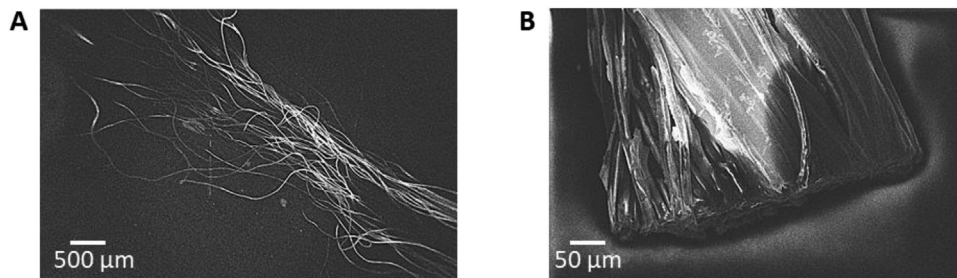


Figure 2. SEM images of: A) As-received PA6 multifilament yarn, B) PEDOT:PSS flow-coated untwisted yarn.

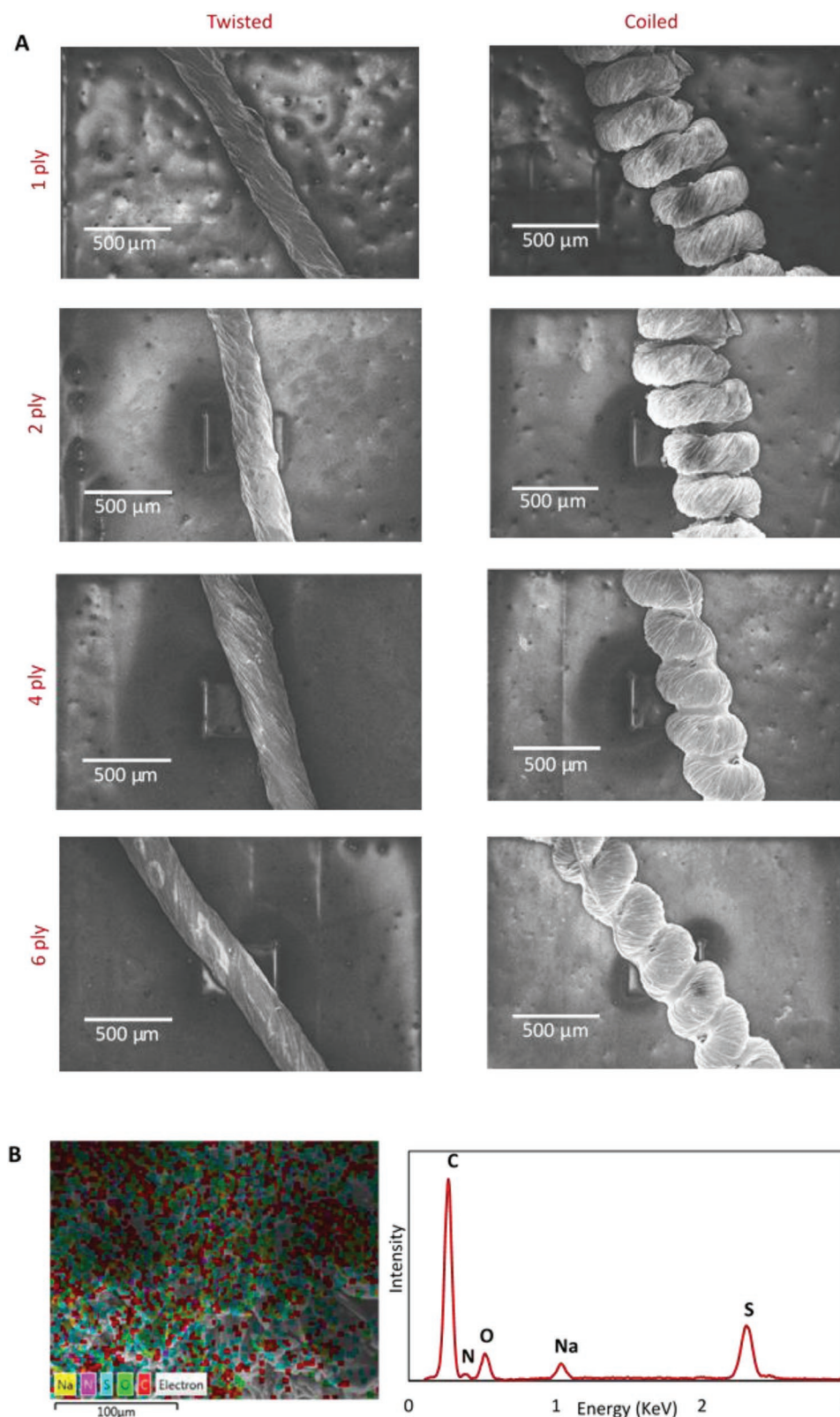


Figure 3. A) SEM images of twisted and coiled yarn actuators made of different core yarn thickness and conductive polymer loading. B) EDX elemental mapping (left portion) and EDX spectra of a sample 2 ply coiled yarn actuators indicating the PEDOT:PSS coating.

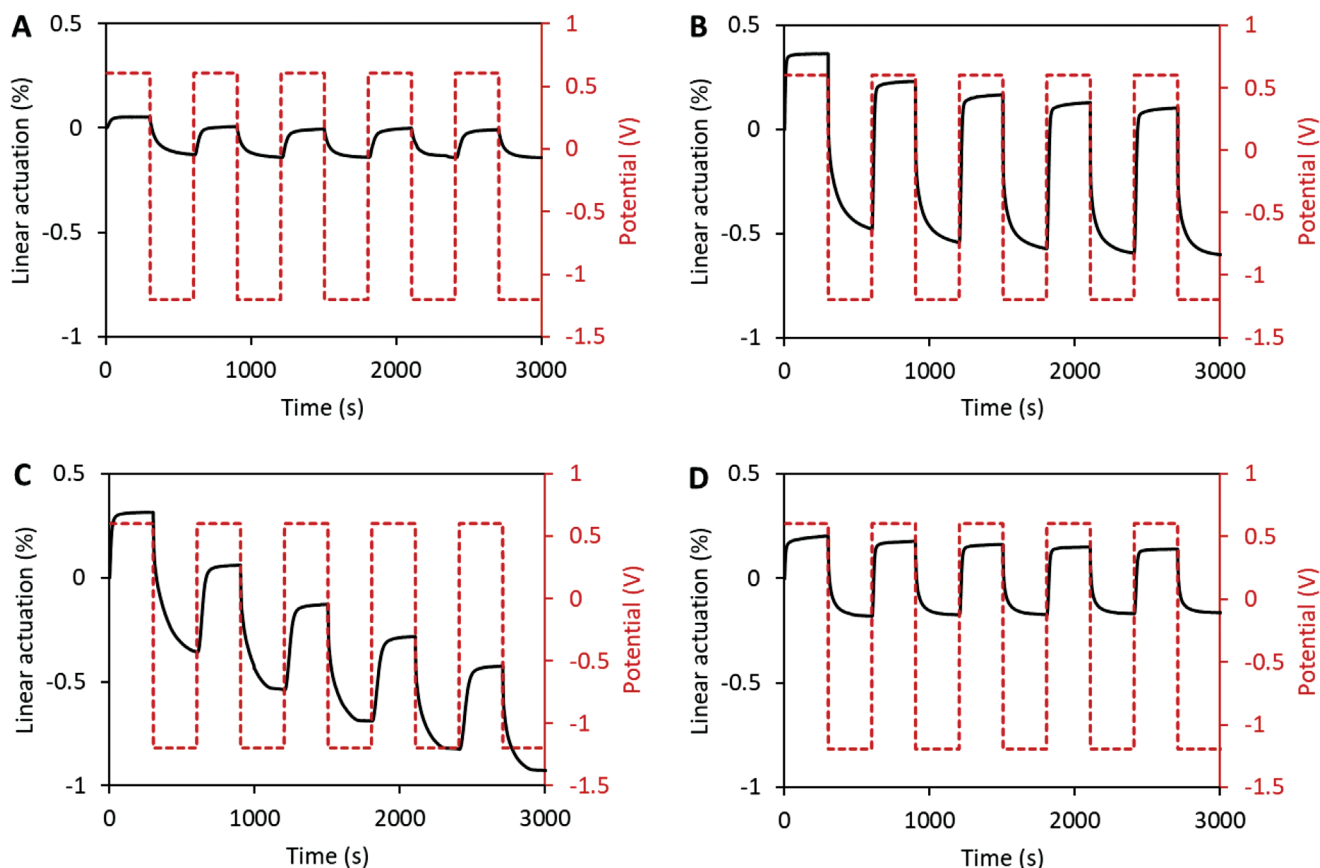


Figure 4. Electrochemically induced linear actuation of twisted yarn actuators biased at 10 mN external force when square potential waves (−1.2 V, 0.6 V vs Ag/AgCl) were applied in 0.1 M NaDBS aqueous solution: A) 1 ply yarn, B) 2 ply yarn, C) 4 ply yarn, D) 6 ply yarn.

(hydrolysis) occurring during the oxidation/reduction cycles^[19] and partially due to a mechanical elastic creep that most materials present when subjected to a mechanical tension.^[20] It was noted that the twisted yarns underwent linear expansion when the positive potential was applied, and a linear contraction when this was reversed to a negative potential. Applying a positive potential oxidizes the PEDOT:PSS coated on and in between the filaments of the twisted yarn in an aqueous NaDBS electrolyte causing significant contraction, and vice versa when the negative potential was applied. Driven by the conformational movements caused by the polymer reduction reaction (Equation 1), Na⁺ cation-driven migration occurs from the solution into the PEDOT:PSS layer to electrically neutralize PSS[−] anions,^[7a] which causes the polymer to expand in the reduced state. Vice versa, oxidation reactions drive the conformational movements allowing Na⁺ cations to be expelled and the PEDOT:PSS contracts. Since the helical structure is initially set by the surface PEDOT:PSS, this contraction/expansion usually causes a partial untwisting/retwisting of twisted yarn actuators that is free to rotate. As in the linear actuation test set-up the yarn actuator was torsionally blocked at both ends and thus exhibited a length expansion/contraction.^[10a] In twisted yarn, the length change in the helical direction due to both PEDOT:PSS volume change and untwisting phenomenon contributed the enhanced linear actuation through the axis of torsionally blocked yarn.

Next, linear actuation measurements of coiled PEDOT:PSS-PA6 yarns in NaDBS electrolyte were conducted by imposing a square potential wave of −1.2 to 0.6 V versus Ag/AgCl, kept each for 300s. **Figure 5** shows five consecutive actuation cycles obtained from coiled yarn actuators made of (A) 1 ply, (B) 2 ply, (C) 4 ply, and (D) 6 ply PEDOT:PSS-PA6 yarn. Reversible linear actuation of 0.21%, 1.62%, 0.37%, and 0.29% was obtained from the twisted muscles made of 1 ply, 2 ply, 4 ply and 6 ply as-received PA6 yarn, respectively. Figure 5 shows that the coiled yarns exhibited linear contraction when the positive charge was applied, and vice versa. As can be seen from Figure 3A, 1 ply and 2 ply coiled yarns yarn actuators have significant gaps in between each individual coil. In this instance, the contraction during oxidation of PEDOT:PSS intended to produce partial untwisting/retwisting of twisted yarn which eventually resulted in length contraction/expansion as a result of the geometrical alteration of blocked yarn untwisting/retwisting. The yarn actuator contraction/expansion has resulted from the combination of this small untwisting/retwisting and the reaction driven volume shrinkage/expansion of the inter-coil PEDOT:PSS polymer. Once oxidized, the shrinkage of PEDOT:PSS allowed the coils to return in their preliminary unstretched length. Reduction of the polymer caused volume expansion and brought the coiled muscle in stretched form. Since the ion-driven PEDOT:PSS exhibits completely reversible volume alteration,^[21] the linear actuation of the coiled muscles has been found to be fully reversible.

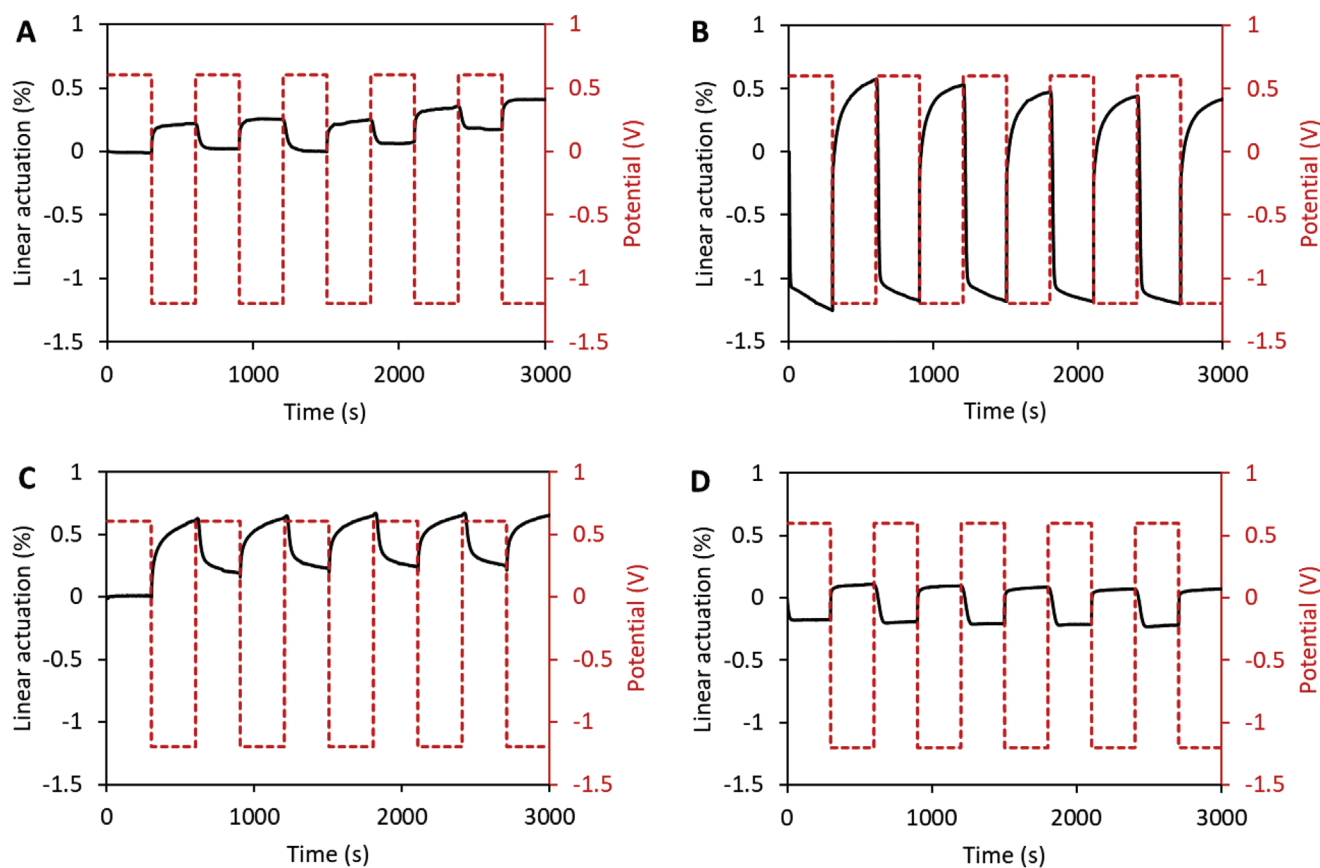


Figure 5. Electrochemically induced linear actuation of coiled yarn actuators biased at 10 mN external force when square potential waves (-1.2 V, 0.6 V vs Ag/AgCl) were applied in 0.1 M NaDBS aqueous solution: A) 1 ply yarn, B) 2 ply yarn, C) 4 ply yarn, D) 6 ply yarn.

Figure 6 shows the linear actuation mechanism of twisted (Figure 6A) and coiled (Figure 6B) yarn actuators, as explained above. Figure 6C shows the comparative linear actuation found from the regular, twisted, and coiled yarn actuators made of 1, 2, 4, and 6 ply as-received PA6 yarns biased at 10 mN external force when square potential waves (-1.2 V, 0.6 V vs Ag/AgCl) were applied in 0.1 M NaDBS aqueous solution. Compared to the untwisted, regular yarns, the twisted 2 ply PEDOT:PSS-PA6 yarn produced 9 \times higher linear actuation. In twisted yarn actuators, the trend in actuation magnitude based on the number of yarn ply can be explained in terms of the torque balance phenomenon compromised by the PEDOT:PSS driven yarn untwisting and the inherent core PA6 yarn resistivity. Starting from the 1 ply yarn, the amount of conductive polymer is significantly less that can withstand the reverse torque present in the core twisted PA6 yarn. Among the samples tested, the yarn actuator composed of 2 ply yarn showed the maximum strain as the result of better balance in between PEDOT:PSS driven untwisting torque and core yarn reverse torque. The use of more yarn plies produced more reverse torque and resulted in less yarn untwisting. Additionally, the increase of core yarn thickness contributed to the increase of overall torsional and tensile stiffness of the yarn actuator which eventually decreased the amount of linear actuation.^[22] Compared to a regular 2 ply yarn, a 2 ply coiled yarn actuator produced >20 \times higher linear actuation. In coiled yarn actuators, the torque balance between

PEDOT:PSS driven yarn untwisting and the inherent core PA6 yarn mechanical resistivity plays an important role in actuation magnitude. The coiled yarn actuators composed of 2 ply yarn showed the maximum strain as the result of better balance in between PEDOT:PSS driven untwisting torque and core yarn reverse torque, in a similar way to the twisted yarns. Coiled yarn actuators made of 4 ply and 6 ply core PA6 yarn also showed linear contraction during oxidation, and vice versa. Unlike the unbiased helical structure of 1 ply and 2 ply coiled yarns, these 4 ply and 6 ply coiled yarns showed the presence of PEDOT:PSS deposited in between each individual coil. This inter-coil polymer further stretches the coiled structure and reduced the untwisting/retwisting amount that is crucial for the linear contraction/expansion.

2.4. Actuation Speed

Next, we investigated the actuation speed by following a previously used method.^[23] Here, the maximum speed of the actuation is provided by absolute reversible strain rates and the times to reach 80% maximum reversible strain. **Figure 7** shows the method of measuring the strain rates, in this case the 2 ply regular (Figure 7A), twisted (Figure 7B) and coiled yarn (Figure 7C) actuators when the potentials ($+0.6$ V, -1.2 V) were applied. The strain rate was obtained by determining the gradient of the

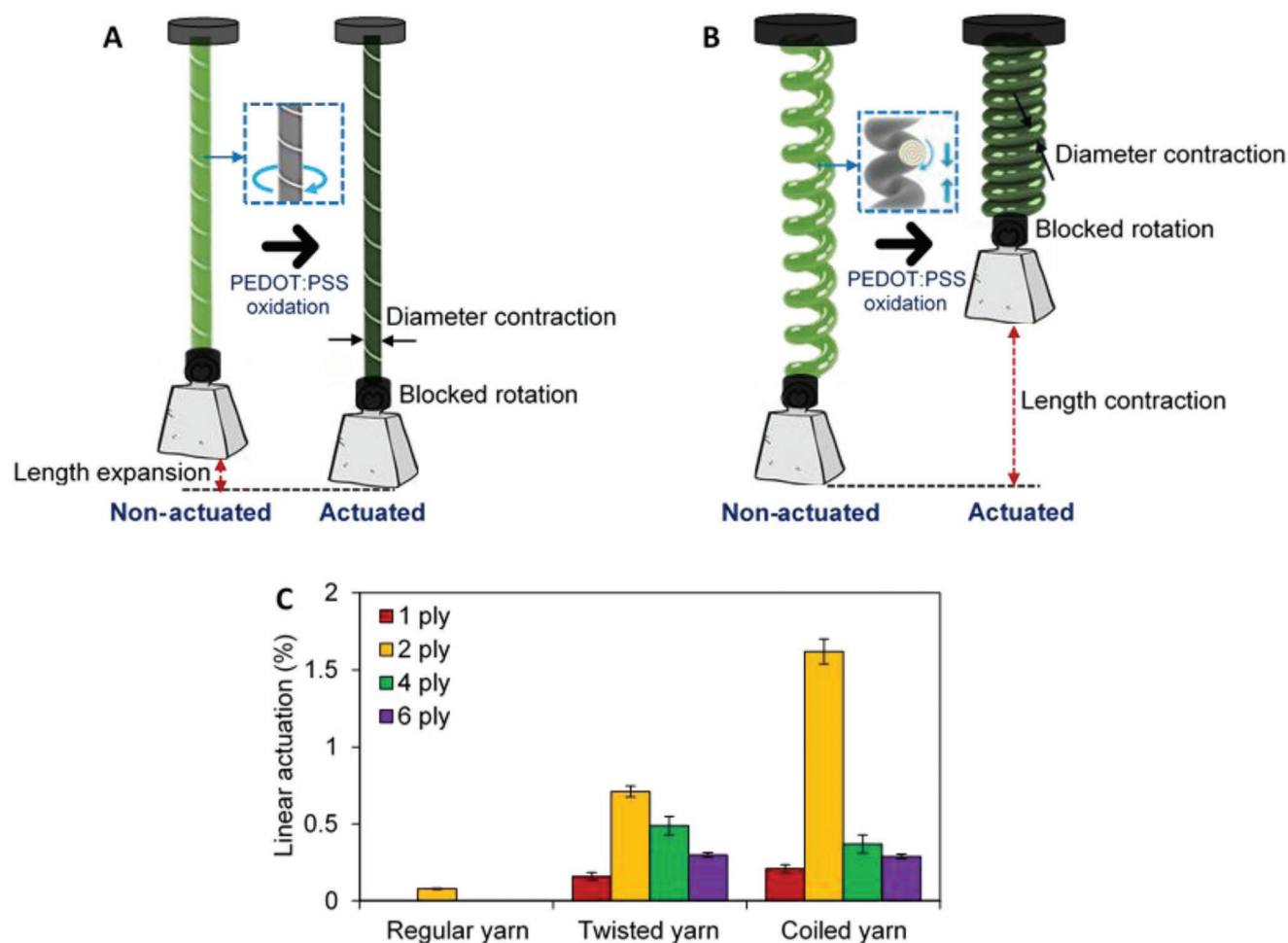


Figure 6. A) Linear actuation mechanism of a twisted yarn actuator. B) Linear actuation mechanism of a coiled yarn actuator. C) Comparative linear actuation results from different yarn actuators: regular/untwisted, twisted, and coiled yarns when square potential waves (-1.2 V, 0.6 V vs Ag/AgCl) were applied in 0.1 M NaDBS aqueous solution.

approximately linear part of the actuation profile during the first part of both oxidation and reduction cycles, this typically being within the first few seconds after switching. The time taken for the muscles to actuate 80% of its maximum value have been extracted considering the maximum strains relative to both oxidation and reduction cycles.

We have extracted the actuation speed of all yarn actuators configurations, twisted, and coiled muscles and for 1 ply, 2 ply, 4 ply and 6 ply PEDOT:PSS yarns (Table 1). For comparison, the actuation speed data for a 2 ply untwisted yarn is also included. For all configurations, the strain rate in yarn reduction step was found to be higher than in oxidation step. Usually, swelling of conductive polymers in an aqueous media are expected to be much faster than deswelling.^[23,24] In aqueous NaDBS electrolyte, PEDOT:PSS swells when reduced, and thus contributing to the faster strain rate. However, the swelling rate near equilibrium swelling is much slower than initial rate due to factors such as material thickness, and diffusion limitations.^[25]

Both the twisted and coiled actuators showed fast electrochemical actuation. For instance, maximum oxidative contraction speed of a 2 ply coiled yarn actuator was found $>32\times$ higher than previously reported polypyrrole/PEDOT:PSS coated yarn

actuator by Escobar-Teran et al.^[9] During reduction, the same coiled yarn actuator showed $>250\times$ higher expansion speed than the reported polypyrrole/PEDOT:PSS coated yarn actuator.^[9] Although the initial strain rates were higher when the 1 ply, 2 ply and 4 ply muscle yarns were reduced, the time taken to achieve 80% actuation were less when they were oxidized. It was also observed that for all samples, the times are longer for oxidation than reduction, confirming previously reported cases.^[23,24] The speed of the muscle yarns also involves a complex micromechanics that relates the change of materials stiffnesses to the actuation force balance. In future works, we will aim to understand these micromechanical properties and relate them to the actuation performance.

3. Conclusion

New types of electrochemically operated yarn-based artificial muscles were prepared by coating multifilament PA6 textile yarns with conductive PEDOT:PSS that provided a great combination of fast and large linear actuation. The PEDOT:PSS-PA6 textile yarns were mechanically twisted and coiled and subjected

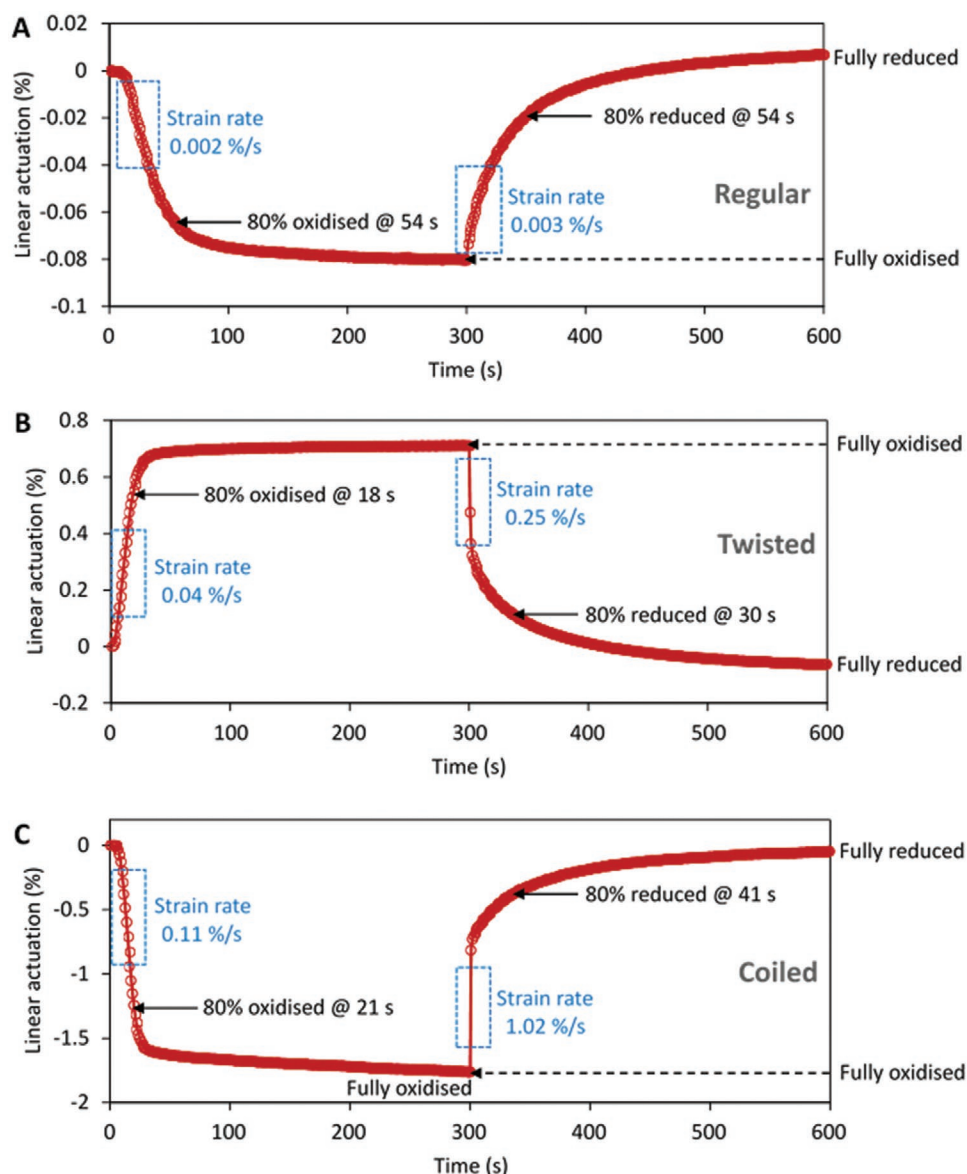


Figure 7. Analysis of actuation speed of 2 ply yarn actuators: A) Regular yarn actuator, B) Twisted yarn actuator, C) Coiled yarn actuator.

to electrochemical actuation tests. The linear actuation was obtained due to a combined mechanism of the cation-driven volume shrinkage/expansion of PEDOT:PSS, helical untwisting/re-twisting of twisted yarns and the conversion of helical rotation to linear movement. Several combinations of core PA6 yarn

thicknesses (1 to 6 ply) and conductive polymer loading were investigated and used to prepare both the twisted and coiled yarn actuators. Among them, twisted and coiled yarns made of 2 ply core yarn produced the highest linear actuation, 0.71% and 1.62%, respectively that was fully reversible. Compared to the

Table 1. Actuation speed of untwisted, twisted and coiled yarn actuators. Here, oxidation and reduction are represented by Ox. and Red., respectively.

Yarn ply	Untwisted yarn actuator				Twisted yarn actuator				Coiled yarn actuator			
	Strain rate [% per s]		Time taken for 80% strain [s]		Strain rate [% per s]		Time taken for 80% strain [s]		Strain rate [%per s]		Time taken for 80% strain [s]	
	Ox.	Red.	Ox.	Red.	Ox.	Red.	Ox.	Red.	Ox.	Red.	Ox.	Red.
1	–	–	–	–	0.004	0.1	41	96	0.006	0.031	15	64
2	0.002	0.003	54	354	0.041	0.25	18	30	0.112	1.023	21	41
4	–	–	–	–	0.022	0.038	23	62	0.015	0.032	33	52
6	–	–	–	–	0.051	0.067	25	16	0.008	0.089	42	13

untwisted, regular yarns, the twisted 2 ply PEDOT:PSS-PA6 yarn produced $>9\times$ higher linear actuation and the coiled yarns produced $>20\times$ higher linear actuation. For coiled muscles, actuation in the reverse direction was noticed which was explained in terms of conductive polymer loading and coil geometry. These muscle yarns are excellent candidates for configuring into textile fabric actuators, and a single yarn outperforms the previously reported yarns for making electrochemically actuated knitted and woven fabrics. For example, obtained strain is a $>21\times$ increase over the polypyrrole coated Lyocell textile yarn from Maziz et al.^[2a] The obtained speed from both twisted and coiled actuators is as high as $>250\times$ faster than the previously reported conductive polymer yarn actuators by Escobar-Teran et al.^[9] The actuation strain and the speed obtained from this work is much higher from the maximum reported results from other electrochemically operated CP yarn actuators, when subjected under similar potential difference (Figure 8).

In this work, we used an aqueous electrolyte since we focused on the enhancement of the yarn actuators themselves. By merging these enhanced yarn actuators with ionogels,^[26] yarn and fabric actuators that operate in ambient air can be constructed to be integrated into actuating textiles.^[27] The use of ionogels, where water is not present, will also partially reduce the creeping effects in actuation strains originating from irreversible side reactions (water hydrolysis) in aqueous electrolytes. Such actuating textiles are of great interest to integrate in active orthoses, augmenting garments, soft exoskeletons and industrial fabrics for instance for the automotive industry.

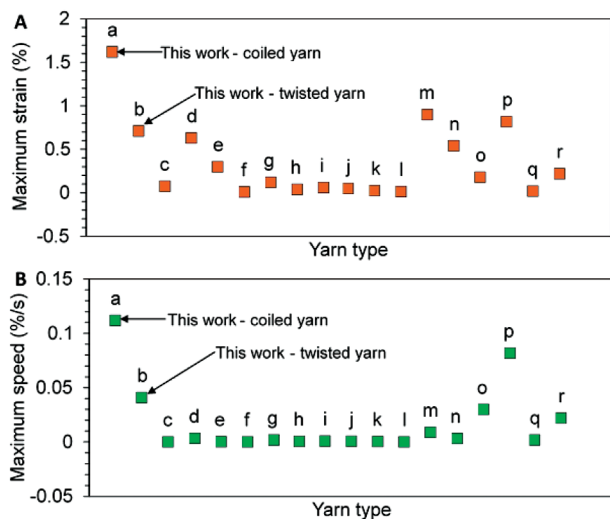


Figure 8. Comparison of A) maximum actuation strain and B) actuation speed of electrochemically activated CP yarn and fiber actuators: a) this work-coiled PEDOT:PSS coated polyamide 6, b) this work- twisted PEDOT:PSS coated polyamide 6, c) polypyrrole/PEDOT coated Lyocell,^[2a] d) polypyrrole/PEDOT:PSS coated Viscose,^[9] e) polypyrrole/PEDOT coated Elastane,^[2a] f) carbon particle mixed polyamide,^[1c] g) carbon particle mixed silicon,^[1d] h) silver coated polyamide,^[1c] i) carbon particle mixed cellulose,^[1c] j) polyester yarn wound with stainless steel wire, k) polyester yarn wound with Sn coated copper wire,^[1c] l) gold coated polyester yarn,^[1c] m) PANI:AMPSA fiber,^[28] n) wet-spun chitosan/polypyrrole microfiber,^[29] o) hollow PPY tubular fiber,^[30] p) Pt wire wrapped PPY hollow fiber,^[30] q) CNT/PPY coated twisted PET yarn^[31] and r) CNT/PPY coated coiled PET yarn.^[31]

4. Experimental Section

Materials: Poly-3,4-ethylenedioxythiophene:poly-styrenesulfonate (PEDOT:PSS) PH1000 from Heraeus Company and dimethyl sulfoxide (DMSO) from Sigma-Aldrich were mixed in a proportion of 60/40 v/v%. Sodium dodecylbenzenesulfonate (NaDBS) from TCI Europe was used as received. Ultrapure water was obtained from Milli-Q Plus water equipment and used for all experiments. PA bulky polyamide 6 (PA6) multifilament yarns from Contifibre were used as received. The multifilament comprises two inter-wrapped ply and each ply contains ≈ 46 monofilaments.

Fabrication of Yarn Actuators: The PEDOT:PSS-PA6 yarn actuators were fabricated by depositing a solution of PEDOT:PSS (60 v/v%) and DMSO (40 v/v%) on the yarn surface (herein called flow-coating) in a two-step process. The complete procedure is illustrated in **Figure 9**. Initially, the solution was gravitationally flown along the surface of as-received bulky PA6 yarns and allowed to dry for 30 min to form a semisolid coating. The amount of solution loading was 250, 500, 1000, and 1500 $\mu\text{L m}^{-1}$ for core 1, 2, 4 and 6 ply yarns, respectively. The as-received yarn is a 2 ply yarn composed of two identical strands of multifilament. Here, 1 ply yarn is one of the two identical strands, 4 and 6 ply yarns are made by wrapping two and three as-received yarns, respectively. Next, the impregnated yarns were mechanically twisted under 10 MPa axial stress until the saturation limit of twist count at which point it started to form coils. The twist induced shear force squeezed the conductive layer and suspended some DMSO onto the yarn surface. The twisted yarns were left stressed for 30 min when the suspended DMSO was reabsorbed by the semisolid conductive polymer. Finally, some of the twisted yarns were further twisted to form coils throughout the length. The uniformity of the coating was maintained while gravity-pulled conductive polymer droplets travelled through the surface of yarns.

Electrochemical and Surface Characterization: All the electrochemical characterizations and electrochemical actuation tests were performed in a single compartment three-electrode electrochemical cell (**Figure 10**), connected to a potentiostat-galvanostat (Autolab PGSTAT204) from Metrohm AG, Switzerland. The input/output parameters were controlled by an electrochemistry software named NOVA 2.1.1. The reference electrode was a BASi MF-2052 Ag/AgCl (3 m NaCl) electrode. All potential values from electrochemical experiments in this work are referred to this electrode. A stainless-steel mesh having 6 cm^2 of surface area was used as the counter electrode. As the electrochemical cell a Falcon tube was used where the tip was cutoff to form an open container. A small hole was drilled in the lid and the yarn was pulled through the hole so that approximately 1.5 cm was kept outside the container/lid. The hole was sealed with epoxy glue to prevent any leakage of the

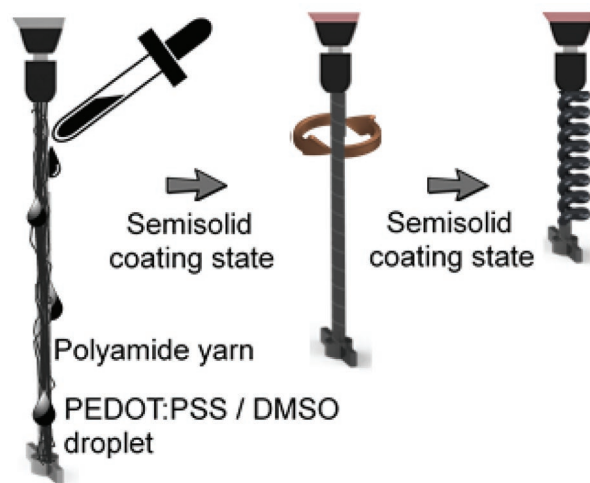


Figure 9. Fabrication steps of twisted/coiled PEDOT:PSS-PA6 muscle yarns.

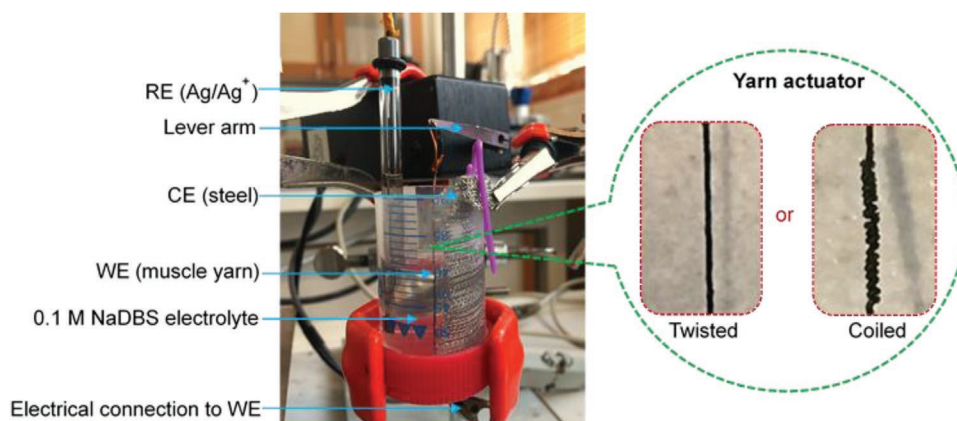


Figure 10. Electrochemical characterization process of twisted and coiled muscle yarns (inset shows the optical images of twisted and coiled muscle yarns).

electrolyte solution. The yarn, now acting as the working electrode (WE) was electrically connected with an alligator clip at this section of the yarn on the outside of the container/lid to eliminate any risks of unwanted side reactions on the metal contact.

CV tests were performed by cycling the potential between 0.6 V and -1.2 V for both twisted and coiled yarns in aqueous 0.1 M NaDBS electrolyte. The qualitative information about electrochemical processes was studied by using 0.01 V s^{-1} scan rate. Length of the yarns was kept constant by connecting them with an isometrically operated force-displacement lever arm transducer (Aurora Scientific model 300B, Canada).

The surface morphology of the yarn actuators was characterized by using optical imaging as well as SEM (Leo 1550 Gemini) operating at 4.00 KeV. EDX spectroscopy was also used to evaluate the elemental presence of on the yarn actuators by using the detector called X-max, manufactured by Oxford Instruments, and Aztec software, operating at 20.00 KeV.

Actuation Tests Procedure: All the experiments were performed at room temperature (22°C). Actuation strains of the yarn actuators were evaluated by using the test-setup shown in Figure 10; however, the lever arm was now operated isotonically. Initially, each type of yarns was connected to the lever arm under a constant force of 10 mN to ensure the samples were held straight. Step potentials (0.6 and -1.2 V) were applied to the electrochemical cell while the lever arm was measuring the real-time contraction/expansion strains. The lengths of the twisted and coiled samples were 60 and 25 mm, respectively, to ensure the consistent yarn length before and after coiling. The time for each contraction/expansion cycle was set for 10 min for all the test samples.

Acknowledgements

J.G.M. acknowledges Promobilia Foundation (F17603) for their financial support. E.W.H.J. acknowledges financial support from the Swedish Government Strategic Research Area in Materials Science on Functional Materials at Linköping University (Faculty Grant SFO Mat LiU No 2009-00971), the Swedish Research Council (2014-3079), Carl Trygger Foundation (CTS:17-215) and European Union's Horizon 2020 research and innovation program under grant agreement no. 825232 "WEAFING." E.W.H.J. thanks the University of Wollongong's Visiting International Scholar Award.

Conflict of Interest

The authors declare no conflict of interest.

Keywords

artificial muscles, conductive polymers, smart textiles, yarn actuators

Received: October 20, 2020

Revised: November 25, 2020

Published online:

- [1] a) J. A. Lee, N. Li, C. S. Haines, K. J. Kim, X. Lepró, R. Ovalle-Robles, S. J. Kim, R. H. Baughman, *Adv. Mater.* **2017**, 29, 1700870; b) J. Park, J. W. Yoo, H. W. Seo, Y. Lee, J. Suhr, H. Moon, J. C. Koo, H. R. Choi, R. Hunt, K. J. Kim, S. H. Kim, J.-D. Nam, *Smart Mater. Struct.* **2017**, 26, 035048; c) J. G. Martinez, K. Richter, N.-K. Persson, E. W. H. Jager, *Smart Mater. Struct.* **2018**, 27, 074004.
- [2] a) A. Maziz, A. Concas, A. Khaldi, J. Stålhand, N.-K. Persson, E. W. H. Jager, *Sci. Adv.* **2017**, 3, e1600327; b) J. Foroughi, G. M. Spinks, S. Aziz, A. Mirabedini, A. Jeiranikhameneh, G. G. Wallace, M. E. Kozlov, R. H. Baughman, *ACS Nano* **2016**, 10, 9129; c) Y. Wu, Y. Yang, C. Li, Y. Li, W. Chen, *Front. Bioeng. Biotechnol.* **2020**, 8, 892.
- [3] a) D. Melling, J. G. Martinez, E. W. H. Jager, *Adv. Mater.* **2019**, 31, 1808210; b) L. Bay, T. Jacobsen, S. Skaarup, K. West, *J. Phys. Chem. B* **2001**, 105, 8492; c) T. F. Otero, J. G. Martinez, *J. Mater. Chem. B* **2016**, 4, 2069.
- [4] a) J. Heinze, B. A. Frontana-Urbe, S. Ludwigs, *Chem. Rev.* **2010**, 110, 4724; b) T. A. Skotheim, J. Reynolds, *Handbook of Conducting Polymers*, Ed. 3, CRC Press, Boca Raton, FL **2007**.
- [5] D. Mantione, I. Del Agua, A. Sanchez-Sanchez, D. Mecerreyes, *Polymers* **2017**, 9, 354.
- [6] a) A. Bund, S. Neudeck, *J. Phys. Chem. B* **2004**, 108, 17845; b) Q. Pei, G. Zuccarello, M. Ahlskog, O. Inganäs, *Polymer* **1994**, 35, 1347.
- [7] a) F. Hu, Y. Xue, J. Xu, B. Lu, *Front. Rob. AI* **2019**, 6, 144; b) H. Okuzaki, S. Takagi, F. Hishiki, R. Tanigawa, *Sens. Actuators, B* **2014**, 194, 59; c) I. Pöldsalu, K. Rohtlaid, T. M. G. Nguyen, C. Plesse, F. Vidal, M. S. Khorram, A.-L. Peikolainen, T. Tamm, R. Kiefer, *Sens. Actuators, B* **2018**, 258, 1072.
- [8] S. Taccola, F. Greco, B. Mazzolai, V. Mattoli, E. W. H. Jager, *J. Micromech. Microeng.* **2013**, 23, 117004.
- [9] F. Escobar-Teran, J. G. Martinez, N.-K. Persson, E. W. H. Jager, *Adv. Intell. Syst.* **2020**, 2, 1900184.
- [10] a) C. S. Haines, M. D. Lima, N. Li, G. M. Spinks, J. Foroughi, J. D. W. Madden, S. H. Kim, S. Fang, M. Jung de Andrade, F. Göktepe, Ö. Göktepe, S. M. Mirvakili, S. Naficy, X. Lepró, J. Oh,

- M. E. Kozlov, S. J. Kim, X. Xu, B. J. Swedlove, G. G. Wallace, R. H. Baughman, *Science* **2014**, 343, 868; b) S. Aziz, G. M. Spinks, *Mater. Horiz.* **2020**, 7, 667.
- [11] a) J. Foroughi, G. M. Spinks, G. G. Wallace, J. Oh, M. E. Kozlov, S. Fang, T. Mirfakhrai, J. D. W. Madden, M. K. Shin, S. J. Kim, R. H. Baughman, *Science* **2011**, 334, 494; b) M. D. Lima, N. Li, M. Jung de Andrade, S. Fang, J. Oh, G. M. Spinks, M. E. Kozlov, C. S. Haines, D. Suh, J. Foroughi, S. J. Kim, Y. Chen, T. Ware, M. K. Shin, L. D. Machado, A. F. Fonseca, J. D. W. Madden, W. E. Voit, D. S. Galvão, R. H. Baughman, *Science* **2012**, 338, 928.
- [12] S. Aziz, S. Naficy, J. Foroughi, H. R. Brown, G. M. Spinks, *Sens. Actuators, A* **2018**, 283, 98.
- [13] a) I. Gualandi, M. Marzocchi, E. Scavetta, M. Calienni, A. Bonfiglio, B. Fraboni, *J. Mater. Chem. B* **2015**, 3, 6753; b) F. Vidal, C. Plesse, D. Teyssié, C. Chevrot, *Synth. Met.* **2004**, 142, 287.
- [14] a) J. G. Martinez, T. F. Otero, E. W. H. Jager, *Phys. Chem. Chem. Phys.* **2016**, 18, 827; b) T. F. Otero, M. Alfaro, V. Martinez, M. A. Perez, J. G. Martinez, *Adv. Funct. Mater.* **2013**, 23, 3929.
- [15] J. Ruiz, B. Gonzalo, J. R. Dios, J. M. Laza, J. L. Vilas, L. M. León, *Adv. Polym. Technol.* **2013**, 32, E180.
- [16] C. S. Haines, N. Li, G. M. Spinks, A. E. Aliev, J. Di, R. H. Baughman, *Proc. Natl. Acad. Sci. USA* **2016**, 113, 11709.
- [17] M. R. Moraes, A. C. Alves, F. Toptan, M. S. Martins, E. M. F. Vieira, A. J. Paleo, A. P. Souto, W. L. F. Santos, M. F. Esteves, A. Zille, *J. Mater. Chem. C* **2017**, 5, 3807.
- [18] S. Mahato, *RSC Adv.* **2017**, 7, 47125.
- [19] L. Valero, J. G. Martinez, T. F. Otero, *J. Solid State Electrochem.* **2015**, 19, 2683.
- [20] J. D. Madden, D. Rinderknecht, P. A. Anquetil, I. W. Hunter, *Sens. Actuators, A* **2007**, 133, 210.
- [21] A. Savva, S. Wustoni, S. Inal, *J. Mater. Chem. C* **2018**, 6, 12023.
- [22] S. Aziz, S. Naficy, J. Foroughi, H. R. Brown, G. M. Spinks, *J. Polym. Sci., Part B: Polym. Phys.* **2016**, 54, 1278.
- [23] D. Melling, S. Wilson, E. W. H. Jager, *Smart Mater. Struct.* **2013**, 22, 104021.
- [24] X. Wang, E. Smela, *J. Phys. Chem. C* **2009**, 113, 369.
- [25] M. J. M. Jafeen, M. A. Careem, S. Skaarup, *Ionics* **2010**, 16, 1.
- [26] a) Y. Zhong, G. T. M. Nguyen, C. Plesse, F. Vidal, E. W. H. Jager, *ACS Appl. Mater. Interfaces* **2018**, 10, 21601; b) Y. Zhong, G. T. M. Nguyen, C. Plesse, F. Vidal, E. W. H. Jager, *J. Mater. Chem. C* **2019**, 7, 256.
- [27] a) N.-K. Persson, J. G. Martinez, Y. Zhong, A. Maziz, E. W. H. Jager, *Adv. Mater. Technol.* **2018**, 3, 1700397; b) R. Granberry, K. Eschen, B. Holschuh, J. Abel, *Adv. Mater. Technol.* **2019**, 4, 1900548.
- [28] W. Lu, E. Smela, P. Adams, G. Zuccarello, B. R. Mattes, *Chem. Mater.* **2004**, 16, 1615.
- [29] Y. A. Ismail, J. G. Martínez, A. S. Al Harrasi, S. J. Kim, T. F. Otero, *Sens. Actuators, B* **2011**, 160, 1180.
- [30] J. Ding, L. Liu, G. M. Spinks, D. Zhou, G. G. Wallace, J. Gillespie, *Synth. Met.* **2003**, 138, 391.
- [31] S. Aziz, J. G. Martinez, J. Foroughi, G. M. Spinks, E. W. H. Jager, *Macromol. Mater. Eng.* **2020**, 305, 2000421.